Impact of the atmospheric climate modes on Mediterranean sea level variability

ARTICLE *in* GLOBAL AND PLANETARY CHANGE · JULY 2014

Impact Factor: 3.71 · DOI: 10.1016/j.gloplacha.2014.03.007

6 AUTHORS, INCLUDING:

Adrián Martínez-Asensio
University of the Balearic Islands

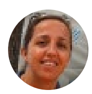

Marta Marcos
Mediterranean Institute for Advanced Studie…

Gabriel Jordà
University of the Balearic Islands

Impact of the atmospheric climate modes on Mediterranean sea level variability

Adrián Martínez-Asensio*[1], Marta Marcos[1], Michael N. Tsimplis[2], Damià Gomis[1], Simon Josey[2], Gabriel Jordà[1]

[1] IMEDEA(UIB-CSIC), Spain

[2] National Oceanography Center, Southampton, UK

*Corresponding author: adrian.martinez@uib.es

Abstract

The relationships of Mediterranean sea level, its atmospherically driven and thermosteric components with the large scale atmospheric modes over the North Atlantic and Europe are explored and quantified. The modes considered are the North Atlantic Oscillation (NAO), the East Atlantic pattern (EA), the Scandinavian pattern (SCAN) and the East Atlantic/Western Russian (EA/WR). The influence of each mode changes between winter and summer. During winter the NAO is the major mode impacting winter Mediterranean sea level (accounting for 83% of the variance) with SCAN being the second (56%) mode in importance. Both NAO and SCAN effects are partly due to direct atmospheric forcing of sea level through wind and pressure changes. However NAO and SCAN are correlated with each other during winter and they explain the same part of variability. The EA/WR also affects the atmospheric sea level component in winter (13%), acting through atmospheric pressure patterns. In winter, the thermosteric contribution is correlated with the SCAN in parts of the Eastern Mediterranean (9%). The rate of change of the thermosteric component in winter is correlated with the EA (24%). During the summer season, the sea level variance is much reduced and the impact of the large scale modes is in most parts of the Mediterranean Sea non significant.

Keywords: Mediterranean, climate indices, sea level variability

1. Introduction

Sea level integrates changes in the thermohaline characteristics of the ocean waters due to heat fluxes and water advection, changes in the ocean mass either due to redistribution of water in response to the atmospheric mechanical forcing or due to the addition or removal of water from the land and the criosphere, and, depending on the reference system, may also include land movements and changes in the oceanic configuration. With the exception of land movements and changes in the shape of the oceanic basin the other two sea level components (thermohaline and mass) are influenced by the large scale atmospheric climate modes through their effect on atmospheric pressure gradients, wind, heat and freshwater fluxes and changes in the oceanic circulation.

Mediterranean sea level rise observed in the longest tide gauges during the last century (1.1-1.3 mm/year) was significantly lower than the global rate (1.5-1.9mm/year) (Tsimplis & Baker 2000; Church and White, 2011). An increase of the averaged atmospheric pressure over the basin during the period 1960-1990 resulted in negative trends of Mediterranean sea level, while in the Atlantic stations the positive trends were lower for this period (Tsimplis & Baker 2000; Tsimplis & Josey 2001). Global and Mediterranean rates significantly increased during the period 1993-2010 (Church and White, 2011; Cazenave et al.2001; Fenoglio-Marc 2001).

For the Mediterranean Sea, the North Atlantic Oscillation (NAO) is known to affect, primarily, winter sea level variability (Tsimplis and Josey, 2001; Gomis et al 2008; Tsimplis and Shaw, 2008; Criado-Aldeanueva et al., 2008; Tsimplis et al, 2013). In addition to dominating the atmospheric component of sea level, a smaller influence of the NAO has also been suggested on the thermosteric component (Tsimplis and Rixen, 2002; Tsimplis et al., 2006; Tsimplis et al., 2013), and on the net evaporation (Tsimplis and Josey, 2001; Mariotti et al., 2002; Fenoglio-Marc et al., 2013) of the Mediterranean Sea. The Mediterranean Oscillation Index (MOI) has been successfully correlated with mean sea level changes, especially during the winter season (Gomis et al 2006; Tsimplis and Shaw, 2008); namely it has been shown to explain 46% of the winter sea level variance for the period 1993-2001 (Suselj et al, 2008). It is worth noting, however, that the NAO index and the MOI are not independent and are significantly correlated in winter.

Raicich et al (2003) found that summer sea level atmospheric pressure in the Mediterranean region is correlated with the Indian monsoon and the Sahel rainfall indices, attributed to particular wind regimes over the area which in turn influenced coastal sea level. Tsimplis and Shaw (2008) identified the East Atlantic pattern (EA) as an additional atmospheric mode impacting sea level, but they only found significant correlations in the Adriatic and once the atmospheric pressure effect was removed. Josey et al (2011) suggested that at least in some parts of the Mediterranean Sea there is a distinct contribution to heat fluxes linked with climatic indices different from NAO, such as the East Atlantic (EA) and the East Atlantic/Western Russian (EA/WR) patterns. In particular they identified correlations between the winter basin averaged heat fluxes and EA, especially at Northwestern Mediterranean and Southern Adriatic, while the correlations between each winter subbasin averaged and EA/WR were in opposite sense in each region, with major values at Aegean Sea. The influence of these modes on heat fluxes necessarily poses the question whether such modes affect at least the steric component of sea level.

The present paper assesses and clarifies the influence of the four major atmospheric modes over the North Atlantic, namely the NAO, the EA the EA/WR and SCAN, on Mediterranean sea level as well as its component driven by wind and atmospheric pressure changes and on the thermosteric component. The analysis is performed for different periods dictated by the availability of tide gauge data and altimetry data. The paper is organized as follows: Section 2 introduces the data sets to represent sea level and its components and the climate indices. In Section 3 we present the methodology of the analysis and in Section 4 we show the main results. Finally, a discussion and some concluding remarks are presented in Sections 5 and 6.

2. Data sets

Sea level observations and estimates of the various contributions to sea level variability have been obtained from the following data sources.

2.1 Tide gauge data

Monthly mean sea level values with benchmark history (Revised Local Reference, RLR) were retrieved from tide gauge records archived at the Permanent Service for Mean Sea Level (PSMSL; Woodworth and Player, 2003). We selected 12 tide gauges distributed along the Mediterranean coasts, each of them spanning more than 35 years of the last decades of the 20th century. The tide gauge stations and their periods of operation are listed in Table 1. Finally, a set of atmospherically-corrected tide gauge records was obtained through removing the atmospheric contribution as given by a sea level hindcast, at the closest grid point to each tide gauge. The VANI2-ERA hindcast used is described later.

2.2. Altimetry data

Gridded Sea Level Anomaly (SLA) fields were obtained from the merged AVISO products available at http://www.aviso.oceanobs.com. The data consist of monthly multimission (up to four satellites at a given time) gridded global sea surface heights spanning the period 1993-2010, with a spatial resolution of 1/4°×1/4°. This version comes with all the standard geophysical corrections applied including the so called Dynamic Atmospheric Correction (DAC; Volkov et al 2007) that accounts for the effect of atmospheric pressure and wind on sea level. This dataset will be referred to as DAC-altimetry. The DAC correction, as supplied by AVISO, was added back to altimetry in order to create a second data set accounting for the atmospheric pressure and wind effects on sea level. This will be called altimetry. Note that because the dataset is a combination of observations from different platforms there is significant uncertainty for the trends derived especially for the last mission. In addition, the applied GIA corrections also introduce significant errors in trends (Ablain et al., 2012). However we do not consider these uncertainties as capable of affecting the correlation with the various atmospheric modes because the variance linked to long term trends is much smaller than the interannual variability analized here.

2.3. Atmospherically-induced sea level

The meteorological contribution to sea level caused by the combined action of atmospheric pressure and wind was quantified from the VANI2-ERA data set (Jordà et al., 2012). VANI2-ERA data are 6-hourly sea surface heights obtained with a barotropic version of the HAMSOM model forced with atmospheric pressure and winds from a dynamical downscaling of the ERA40 reanalysis. The data span the period 1958-2008 and cover the Mediterranean Sea and a sector of the NE Atlantic Ocean with a spatial resolution of 1/6°×1/4°. Two additional runs were also performed: one forced only by wind and the other forced only by atmospheric pressure variations. Model hourly outputs were converted into monthly fields at each grid point.

2.4. Hydrographic data and thermosteric sea level

Ocean temperature (T) fields from Ishii and Kimoto (2009; version 6.12) were used to compute thermosteric sea level in the Mediterranean Sea (download website: http://rda.ucar.edu/datasets/ds285.3/). The data set consists of monthly T fields over a 1ºx1º global grid down to 1500m and spanning the period 1950-2011. Thermosteric sea level was computed at each grid point over the Mediterranean Sea by vertically integrating the specific volume anomaly at each grid cell down to 300 m. The reference level at 700 m was also sued for comparison, but the results did not differ. Therefore the 300 m reference level was preferred because there are a higher number of observations at upper levels. Depths deeper than 700 m were not considered due to the scarcity of observations. Salinity (S) values are also available in the same dataset. However, because S measurements are highly sparse and uncertain over the entire basin (Jordà and Gomis, 2013), thermosteric sea level was preferred instead of steric sea level. For the calculation of the thermosteric height changes S was considered constant to the 1950 value at each depth.

2.5 Atmospheric variables

Mean sea level atmospheric pressure, 2m air temperature, net heat fluxes and 10m wind velocity, were obtained from NCEP/NCAR atmospheric reanalysis (Kistler et al., 2001). We used monthly mean values obtained from the 6h output fields with a spatial resolution of 2.5ºx2.5º over the period 1950-2011.

2.6. Climate indices

The leading atmospheric climate modes used, namely NAO, EA, EA/WR and SCAN, as computed for the period 1950-2011 were downloaded from the NOAA Climate Prediction Centre (http://www.cpc.ncep.noaa.gov/data/teledoc/telecontents.shtml). These modes were obtained through a rotated principal component analysis (Barnston and Livezey, 1987) of the monthly mean standardized 500-mb height anomalies in the Northern Hemisphere. This ensured that they are orthogonal (independent) to each other at a monthly scale. The source of the data is the same as that used by Josey et al (2011) although the period covered in this study is longer. Our approach has considered the sea level impacts of the four leading modes of atmospheric variability that have an influence in the Mediterranean Sea region as identified by the NOAA Climate Prediction Centre analysis. Other patterns can be defined but they are likely to reflect a combination of the modes that we have already employed. Hence, our focus has been on these four modes. Future research that considers Mediterranean sea level impacts of other patterns of variability should be careful to identify the extent to which the other patterns are dependent on those already considered here.

3. Methodology

Winter and summer averages, defined as the mean values over the period December to March and June to August, respectively, were computed for each climate index. The correlations among the seasonal averages of the climate indices used are listed in Table 2. The NAO and SCAN are anticorrelated in winter. In the summer the EA, EA/WR and SCAN are all correlated with each other.

Composite fields of 2m air temperature, sea level pressure and wind anomalies were used to develop spatial patterns of the relevant atmospheric field corresponding to the high and low values of each index. The composite fields were built as follows: first, monthly fields of the atmospheric variables coinciding with a climate index larger than 1.5 (or lower than -1.5) were selected. Each monthly field was then multiplied by the corresponding index value and the resulting time series was weighted averaged. The pattern obtained in this way can be considered associated with a unit positive value of the climate index. Using different thresholds for the climate indices did not alter significantly the results. The resulting patterns for the positive phase of each index are shown in Figure 1.

Seasonal averages were calculated for the tide gauge records for the period December to March (winter) and for the period June to August (summer). For the gridded data, seasonally basin averaged time series, for the same periods, were obtained by calculating averages over the whole Mediterranean basin as well as over the eastern and western sub-basins (the Sicily Strait has been used as the separation line between the eastern and western basins). Seasonal variances of the different data sets are listed in Table 3. The values correspond to the basin averaged variance and its standard deviation. The lowest and highest value for each data set is also shown for comparison.

All time series were detrended and the seasonal cycle was removed before the regression analysis. The relationship between the various climate indices and sea level was explored on the basis of the correlation and linear regression values between the seasonal (winter and summer) anomalies of each variable and the corresponding seasonal time series of each index. The trend removed corresponded to the common period of the time series and the corresponding index. Significance was set at the 95% level.

Multiple linear regression analysis was, in addition, performed with sea level or one of its components as the dependent parameter and all four indices as independent parameters. Note that the correlation between the seasonal values of the indices (Table 2) indicates that there is the possibility that the same variance in sea level can be accounted for by more than one index. Forward stepwise multiple linear regression analysis (Draper and Smith, 1998) was used to select the statistically significant contributors. This procedure selects the most correlated dependent variable and removes its influence through a regression analysis. Then it checks for correlation between the rest of the dependent parameters and the residual signal, until the correlation becomes non-significant. Where more than one index can account for the same part of variability the regression model favours the index that accounts for the highest percentage of total variability.

4. Results

4.1. Observed sea level from tide-gauges

Correlations between seasonal climate indices and tide gauge records and atmospherically corrected tide gauge records are shown in Figure 2. For some of the indices significant differences can be found between eastern and western basins. The winter NAO is found to be correlated with observed winter sea level at all sites. In the Adriatic it was also correlated during summer at most stations. SCAN was positively correlated during winter in the Adriatic stations as well as in Marseille and Genova. These similarities are in agreement with the negative correlation of -0.47 found between winter NAO and SCAN (Table 2). EA/WR was correlated with sea level during winter, in the Adriatic Sea and Alexandria at the Eastern Mediterranean. The removal of the atmospheric forcing component using VANI2-ERA hindcast reduced the correlation coefficients but did not make the correlations statistically insignificant.

During the summer season the NAO is correlated with sea level in some Adriatic stations. The EA is correlated in the Adriatic stations and Genova. The removal of the atmospheric forcing component increased the correlation with the EA in the Adriatic.
The variance accounted for by the indices at each tide gauge record and the corresponding atmospherically corrected tide gauge record are listed in Table 4. The results of the regression analysis against the four modes are shown at Table 4. The results for the multiple regression are shown in parenthesis. Note that although SCAN accounts for a significant amount of the variance for the Adriatic stations and Genoa and Marseille in the multiple regression model it is considered redundant by the selection process at most of the tide gauges except in Venice and Rovinj. This is probably a consequence of the inter-dependence of winter averaged NAO and SCAN.

The results of multiple regression indicate that the NAO is the leading mode for winter sea level in the Mediterranean Sea, accounting for 13% to 47% of the variance of observed sea level and for 7% to 26% of the variance of atmospherically corrected sea level. The EA/WR accounts for 6% to 22% in the Adriatic and the eastern sub-basin and conserves similar values when the atmospheric correction is applied (8% to 19%). The EA accounts for 6%-18% of the variance of corrected sea level. Overall, the climate indices account for 39%-56% of the total inter-annual sea level variability in winter and for 14%-41% when the atmospheric correction is applied. The multiple regression models are shown in Fig.3.

During summer the influence of climates modes in sea level variability from tide gauges is smaller. In the Adriatic the NAO accounted for 13% to 15% of the variance. The correlation with the other indices seems random (Table 4 and Figure 3). However, the summer EA accounts for 8% to 16% of the variance at Genova, Marseille and the Adriatic tide gauges when the atmospheric contribution is removed.

4.2. Observed sea level from altimetry

Statistically significant winter correlations between the climate indices and altimetry are mapped in Figure 4 (left column). The corresponding basin averaged correlation and the variance accounted for is listed in Table 5. Summer maps are not shown because no statistically significant correlation has been identified. The correlations with tide gauges, but computed for the same period as the altimetry are also mapped for completeness (Figure 4, left). The highest correlation for basin average was found between altimetry and NAO (-0.91). The correlation with SCAN was slightly lower (0.75).
The multivariate regression model selects the NAO as the independent parameter while the SCAN mode becomes redundant. For this reason the variance accounted for by SCAN is zero in Table 5. The winter NAO accounts for 77% of the variance followed by EA/WR (7%) (Table 5 and Figure 5 top). These values are consistent with the variances of tide gauges accounted for by the indices. However, the NAO accounts for more variance during the altimetric period than for the tide-gauge period whereas the opposite is true for EA/WR. Note that the EA/WR correlations are below the significance level for most of the domain. Nevertheless it accounts for a small fraction of the variability. The multiple regression model accounts for 83% of the basin averaged winter variance of sea level.

Winter correlations between climate indices and DAC-altimetry are represented in Figure 4 (right). The correlations with atmospherically corrected tide gauges are also mapped over the DAC-altimetry maps. Basin and sub-basin averages of correlations and variances accounted for by the indices according to the multiple regression model are listed in Table 5. No significant correlations were found in summer (not shown). The highest correlation (in absolute values) was obtained with NAO (-0.9) SCAN having the second largest (0.6). The correlation with EA was also significant over part of the western sub-basin, with an average value of 0.5.

The multiple regression model considered SCAN redundant. The contribution of each independent mode to winter atmospherically-corrected sea level variability averaged over the entire basin is represented in Figure 5 (bottom), being the NAO the only significant mode, accounting for 78% of the variance. In the western sub-basin EA accounted for around 12% of the variance.

It is worth to clarify that the difference in winter variances found between tide gauges (32±10 cm2) and altimetry (19±7 cm2) listed in Table 3 is attributed to the different periods considered and to the fact that the altimetry average covers the whole basin, while the tide gauge value is point-wise. Indeed, when the winter variance of altimetry is calculated by averaging only the closest grid points to tide gauges and limiting the tide gauge average to the altimetry period this difference is significantly reduced (11±4 cm2 and 14±9 cm2, respectively).

4.3 Atmospherically forced sea level

Seasonal correlations between climate indices and atmospherically-induced sea level as given by the barotropic hindcast forced by pressure and wind are mapped in Figure 6 for winter (a-d) and summer (i-l). Basin averaged correlations and the corresponding variances accounted for are listed in Table 6. With the exception of the EA, all other are correlated with the winter atmospheric component of sea level. The highest correlation (-0.7) is with NAO. For the winter season about 50% of the variance is accounted for by the NAO index and 11% by the EA/WR. The correlation with SCAN was found redundant.

Overall the variance accounted for by the climate modes was about 60%. The statistical model for the averaged basin sea level for the NAO alone and the NAO and EA/WR are shown in Figure 7 (top).

It must be remarked however, that the atmospherically-induced sea level variability is much smaller in summer than in winter; thus, the impacts of the climate modes are also smaller in absolute terms.

During summer, SCAN explains 14% of the variance; the other modes do not show statistically significant correlations (Table 6). Despite the low correlation obtained with NAO (-0.19 over the basin), this mode accounts for 8% of the variability in the eastern sub-basin, according to the regression model. The corresponding time series of the summer atmospherically-induced sea level and the regression model are plotted in Figure 7 (bottom).

Regression and correlation analysis was also performed for wind-only and pressure-only forced sea level (Table 6). Seasonal correlations for wind-only forced sea level are mapped at Figure 6 for winter (e-h) and summer (m-p). During winter, the NAO is the leading mode for wind and pressure only forced sea level with very similar basin averaged correlations (–0.67 and 0.68) and corresponding variances accounted for between 45% and 49%.

For the multiple regression model of pressure-only forced sea level all four independent modes contribute to winter basin-averaged sea level variability, reaching an overall value of 60%.

For the multiple regression model for wind-only forced sea level the EA/WR is the only pattern which, together with NAO, contributed to the winter variance (51%). Although both EA and SCAN were correlated with wind sea level component at western subbasin and overall the basin, respectively, they were considered redundant.

Results for the summer season are different. The pressure only forced sea level is correlated with NAO at some areas of northern Adriatic and at 20-30ºE area of Eastern sub-basin, while SCAN is correlated at western sub-basin. Interestingly, sea level forced by wind only in summer is correlated only to the EA mode in almost all of the basin. However the variance accounted for is only 9%.

4.4 Thermosteric sea level

Thermosteric sea level has much smaller variance than the observed sea level and the atmospherically-corrected sea level (Table 3). Thus any significant correlation found should be interpreted in this context.

The results for winter correlations between climate indices and thermosteric sea level are represented in Figure 8 (left) and Table 7. During winter, SCAN is the index that displays higher correlation, concentrated over the central and eastern regions of the Mediterranean, with an average value of 0.30. SCAN explains about 9% of the winter basin averaged thermosteric sea level variance. NAO is also correlated with the thermosteric sea level over a fraction of the eastern sub-basin. The time series of the averaged thermosteric sea level and the resulting regression models are plotted in Figure 9. No significant correlations were found for the summer.

Changes in thermosteric sea level, at each part of the basin, result from atmospheric heat fluxes and lateral heat advection. Significant correlation (0.59) was found between net heat fluxes and the seasonal average of the time derivative of thermosteric sea level (0.59) averaged over the basin for the period 1950-2008. Note that the seasonal average of the time derivative of thermosteric sea level is the change in thermosteric sea level between November and March divided by four, and between August and May divided by three. The correlations with indices during winter and summer are mapped in Figure 8 (center and right columns) and the averaged correlations and variances accounted for are listed in Table 7. During winter, only EA is correlated over most of the western sub-basin and over the Adriatic with an average value of 0.49 over all the basin. EA/WR shows correlations in the most western and eastern parts of Mediterranean. However, the averaged values have opposite sign depending on the sub-basin (0.30 and -0.22, respectively). SCAN show correlations only in the central parts of the eastern sub-basin (0.30). EA is the only mode that explains part of the variance of the winter basin averaged rate of change of thermosteric (17%). However, combined with EA/WR account for a 21% of the variability of the basin, while combined with EA/WR and SCAN account for the 23% of the eastern averaged. These results are consistent with Josey et al (2011) who showed that EA is the mode driving air-sea net heat fluxes variability over the Mediterranean, especially over western sub-basin, while the NAO and SCAN play much smaller role; EA/WR also plays an important role, but generates a dipole with opposite signal on western and eastern sub-basins. During summer only EA/WR is correlated with thermosteric rate of change at the south part of the eastern sub-basin, however it is correlated with the basin averaged (-0.35) accounting for 12% of the variance. SCAN appears correlated at southern part of the western sub-basin (-0.29), where it explains about 9% of the variance.

5. Discussion

The Mediterranean Sea level variance is larger in winter than in the summer. According to altimetry it is about three times larger; according to coastal tide gauge records it is about five times larger. The statistical modelling of this variance on multiple regression models both for tide gauges and altimetric data show that the NAO can account for most of the winter variability. The use of the atmospherically forced sea level hindcast shows that the NAO influence is due both to the atmospheric pressure forcing and to wind forcing. The sea level correlation with the NAO remains after the DAC correction is applied. This means that the NAO influence on the Mediterranean is not restricted to the local atmospheric pressure and wind effects.

Although SCAN and NAO are monthly independent, they are correlated in winter. All modes show influence in the pressure driven part of the atmospheric forcing, hardly surprising as they are determined on the basis of pressure changes. However only the NAO and SCAN are correlated with the wind driven part of sea level in the winter. The EA is the only mode influencing the wind driven sea level in the whole of the Mediterranean Sea during the summer season.

The relationship between thermosteric sea level and the other large scale climate modes considered in this study is not clearly demonstrated and the results found are spatially restricted to certain areas. Changes in the seasonally averaged rate of change of the thermosteric sea level can be partly accounted for by the EA (21% in winter and 12% in summer) but with differences between the western and eastern sub-basins.

The physical mechanisms through which the atmospheric climate modes impact on Mediterranean sea level and its contributions can be discussed further using composite maps of anomalies of sea level components, wind speed and mean sea level pressure for each pattern corresponding to index values higher than 1.5 or lower than -1.5.

Figure 10 shows the composite maps of atmospherically forced winter sea level during the positive and negative NAO phases and the corresponding map for EA/WR, the only two indices we found accounting for the variance in the relevant multiple regression model. Note that pressure and winds mapped here are not anomalies as in Figure 1. The spatial pattern of the atmospheric component of sea level reflects that of the atmospheric pressure: during a positive phase atmospheric pressure displays a meridional gradient with lower values in the eastern sub-basin mimicked by the sea level response. On the contrary, during a negative NAO phase, atmospheric pressure is lower and more homogeneous within the basin and consequently sea level values are higher. The winds associated with the NAO mode contribute in the same sense than atmospheric pressure to the atmospherically-induced winter sea level. Fukumori et al. (2007) have shown that winds around the Strait of Gibraltar can produce significant basin-wide oscillations in the Mediterranean. Winds associated to the NAO negative phase are prone to induce a net mass flux through the Strait of Gibraltar, so inducing a sea level increase in the basin (Fukumori et al., 2007).

The second mode correlated with winter sea level and its atmospheric component, in the multiple regression model, was the EA/WR. This mode was not significant for the atmospherically-corrected sea level (Table 5), indicating thus that the influence on sea level was exclusively through the atmospheric pressure and the local wind forcing. Wind anomalies composites (Figure 1) suggested that positive phases of EA/WR favour northerly strong winds, over the eastern basin. During a positive phase of EA/WR, the atmospherically-induced sea level associated with this mode displays an E-W gradient in response to the atmospheric pressure pattern over the Mediterranean (Figure 10c). During the negative phase of EA/WR (Figure 10d), the spatial pattern of atmospherically-induced sea level is more uniform and dominated by westerly winds.

In Figure 11 composite maps for the anomalies in the rate of change of thermosteric sea level are shown. As seen previously (Fig. 8), the NAO is only correlated with parts of the Eastern Mediterranean. The winter EA is the mode most closely correlated with the rate of change of thermosteric sea level. This is despite the fact that the EA does not correlate with atmospherically-induced sea level in general but does correlate with the wind driven part of the sea level. The underlying correlation between the wind field over the Mediterranean and the EA is important for the heat fluxes. In its positive phase, EA is characterized by an atmospheric pressure anomaly pattern with very weak gradients over the Mediterranean Sea and the nearby Atlantic (Figure 1). The circulation associated with the positive EA state involved westerly winds coming from the Atlantic, while the negative phase northerly winds coming over the Gulf of Lions, in agreement with the results presented by Josey et al (2011). As heat fluxes are always negative in winter, this translates into smaller than average heat losses, especially over the western sub-basin (Figure 11c). Likewise, the EA negative phase in winter is associated with northerly winds and colder air T, resulting in larger than average ocean heat losses and more negative anomalies of the rate of change of thermosteric sea level (Figure 11d). The rates of change of thermosteric sea level were found to be also related with EA/WR and SCAN at some areas of the basin (Table 7 and Figure 11). The associated with EW/WR winter wind fields show that during the positive phase of EA/WR northerly winds bring cold air over some areas of the eastern sub-basin resulting in a higher than normal heat loss (Figure 11e) while in the western part of the basin winds coming from the west contributes to a lower than normal heat loss. The opposite effect occurs during the negative phase of EA/WR, when a westerly flow of warmer air contributes to decreasing the rates of change of the thermosteric component (Figure 11f). The positive phase of SCAN is associated with a westerly flow of warm air that induces lower than normal decreasing of thermosteric sea level, mostly over the central-eastern Mediterranean. In its negative phase, there is a pattern of warmer north-westerly winds due to the absence of the low-pressure conditions over the western sub-basin and the result is a much lower decreasing of thermosteric sea level than in the positive phase.

During the summer season, SCAN was the only relevant mode for summer atmospherically-induced sea level, accounting for only 14% of the variance (1.0±0.2 cm2) on average over the basin. Figure 12a and 12b show that the mechanism through which the SCAN pattern impacts on the atmospheric contribution is its associated atmospheric pressure pattern for both the positive and negative phases, as the atmospherically-induced pattern follows that of the atmospheric pressure. EA/WR and, to a lesser extent, SCAN patterns influenced the rates of change of thermosteric sea level during summer. For both positive and negative phases, EA/WR induce northerly winds over the Mediterranean (Figure 12c, d); however, air T over Europe is colder (warmer) than average during the summer positive (negative) phase (not shown), which explains lower (higher) rates of change of thermosteric sea level.

6. Conclusions

The four independent large scale modes dominating the atmospheric variability over the North Atlantic and Europe (NAO, EA/WR, SCAN and EA), impact differently on sea level and its components. Table 8 summarizes the results presented throughout the paper for each sea level contribution.

The major conclusions of this work are summarized in the following:

- The NAO is the main mode in terms of impacts on winter Mediterranean sea level variability (-5.6 cm of altimetry sea level per unit NAO with a correlation of -0.91) as a result of two physical processes that contribute to amplify the atmospheric signal: i) the direct forcing of atmospheric pressure and wind within the basin (-2.9 cm per unit NAO with a correlation of -0.71) which induces changes in the flux through Gibraltar, and ii) the forcing of Gibraltar mass exchanges caused by winds near the Strait. In addition Calafat et al. (2012) demonstrated that wind driven baroclinic circulation in the Atlantic also impact on Mediterranean sea level. Positive/negative winter NAO phases induce lower/higher Mediterranean sea level as a result of these two mechanisms.

- The SCAN pattern is significantly correlated with winter Mediterranean sea level (0.89). However, it has been found to be redundant with winter NAO, as the atmospheric patterns associated with these two modes are very similar over the Mediterranean (confirmed by the correlation between winter NAO and SCAN modes). Otherwise, SCAN is the only mode that contributes to the winter thermosteric sea level with 0.4 cm per unit index.
- EA/WR is the second large scale mode in importance for Mediterranean sea level (-2.2 cm of altimetry sea level per unit index and a correlation of -0.36) , and acts mainly by forcing the atmospheric sea level component, more particularly by atmospheric pressure changes.
- The EA mode impacts on the rate of change in winter thermosteric sea level.
- In summer the variance of atmospherically induced sea level is much lower than in winter (1.0±0.2 cm2). SCAN is correlated with atmospheric summer sea level (0.38, 0.6 cm/unit) and the effect is solely attributed to pressure. The EA is the only mode that contributes to the wind-only induced sea level (-0.31) with -0.2 cm per unit index but the correlation is not significant for the atmospheric component as a whole or for the observed sea level.

This work demonstrates that the study of the large-scale atmospheric variability can help to understand sea level changes at a regional scale, at least for some of the sea level components. Most notably, this is the first study that offers a complete overview of the relationships between the major large-scale atmospheric patterns and Mediterranean sea level and its components over the last decades. Our results provide both the relative and overall contribution of atmospheric patterns to sea level variability in Mediterranean Sea, an information that could be used for the study of past and future scenarios.

Acknowlegdments

This work has been carried out in the framework of the projects VANIMEDAT-2 (CTM2009-10163-C02-01, funded by the Spanish Marine Science and Technology Program and the E-Plan of the Spanish Government) and ESCENARIOS (funded by the

Agencia Estatal de METeorología). A. Martínez-Asensio acknowledges an FPI grant associated with the VANIMEDAT-2 project, M. Marcos acknowledges a “Ramón y Cajal” contract funded by the Spanish Government and G. Jordà acknowledges a JAE-Doc contract funded by the Spanish Research Council (CSIC) and the European Science Foundation. We are grateful to Météo-France for providing atmospheric reanalyses. Finally we thank A. Sánchez-Román for his comments and data providers such as AVISO for providing altimetry data, PSMLS for tide gauges data and NOAA for the climate indices and the atmospheric reanalysis. We thank Piero Lionello and another anonymous reviewer for their constructive comments.

References

Ablain, M., Philipps, S., Urvoy, M., Tran, N. and Picot,N., 2012. Detection of Long-Term Instabilities on Altimeter Backscatter Coefficient Thanks to Wind Speed Data Comparisons from Altimeters and Models. Marine Geodesy 35:sup1, 258-275

Barnston, Anthony G., Robert E. Livezey, 1987. Classification, Seasonality and Persistence of Low-Frequency Atmospheric Circulation Patterns.Mon. Wea. Rev., 115, 1083–1126.

Calafat, F. M., G. Jordà, M. Marcos, and D. Gomis, 2012. Comparison of Mediterranean sea level variability as given by three baroclinic models, J. Geophys. Res., 117.

Cazenave A., Cabanes, C., Dominh, K. & Mangiarotti, S., 2001. Recent sea level changes in the Mediterranean Sea revealed by TOPEX/POSEIDON satellite altimetry, Geophys. Res. Lett., 28(8), 1607–1610.

Church, J. A. and N.J. White, 2011. Sea-level rise from the late 19th to the early 21st Century. Surveys in Geophysics, 32, 585-602.

Criado-Aldeanueva, F., Del Río Vera, J., García-Lafuente, J., 2008. Steric and mass-induced Mediterranean sea level trends from 14 years of altimetry data, Global and Planetary Change, 60, 3–4.

Draper, N. R. and Smith. H., 1998. Applied Regression Analysis. Hoboken, NJ: Wiley-*Interscience, 1998. pp. 307–312.*

Fenoglio-Marc, L., 2001. Analysis and representation of regional sea-level variability from altimetry and atmospheric–oceanic data. Geophys. J. Int., 145. 1–18.

Fenoglio-Marc, L., Mariotti, A., Sannino, G., Meyssignac, B., Carillo, A., Struglia, M.V., Rixen, M. 2013. Decadal variability of net water flux at the Mediterranean Sea Gibraltar Strait, Global and Planetary Change, 100, 1-10.

Fukumori , Menemenlis, D. and Lee, T. 2007. A Near-Uniform Basin-Wide Sea Level Fluctuation of the Mediterranean Sea. Journal of Physical Oceanography 37:2, 338-358

Gomis, D., Tsimplis, M.N., Marcos, M., Fenoglio-Marc, L., Pérez, B., Raicich F., Vilibić I., Wöppelmann, G., Monserrat S., 2011. Sea Level Rise and its Forcing in the Mediterranean Sea. In: The Mediterranean climate from the present to the future, Lionello P. (ed.), Elsevier.

Gomis, D., S. Ruiz, M. García-Sotillo, E. Álvarez-Fanjul, and J. Terradas 2008. Low frequency Mediterranean sea level variability: The contribution of atmospheric pressure and wind, Global Planet. Change, 63, 215-229.

Ishii, M. and M. Kimoto, 2009: Reevaluation of Historical Ocean Heat Content Variations With An XBT depth bias Correction. J. Oceanogr. 65, 287299, doi:10.1007/s10872-009-0027-7.

Jordà, G., Gomis, D., Álvarez-Fanjul, E., 2012. The VANI2-ERA hindcast of sea-level residuals: Atmospheric forcing of sea-level variability in the Mediterranean Sea (1958-2008). Scientia Marina, 76, 133-146.

Jordà, G., Gomis, D., 2013. Reliability of the steric and mass components of Mediterranean sea level as estimated from hydrographic gridded products. Geophys. Res. Letters (40) 1–6, doi:10.1002/grl.50718

Josey, S. A., Kent, E. C. and Sinha, B. 2001. Can a state of the art atmospheric general circulation model reproduce recent NAO related variability at the air-sea interface?,Geophys. Res. Lett., 28, 4543-4546.

Josey, S. A., S. Somot, and M. Tsimplis. 2011. Impacts of atmospheric modes of variability on Mediterranean Sea surface heat exchange, J. Geophys. Res., 116, C02032, doi:10.1029/2010JC006685

Kistler, R., E. Kalnay, W. Collins, S. Saha, G. White, J. Wollen, M. Chelliah, W. Ebisuzaki, M. Kanamitsu, V. Kousky, H. van den Dool, R. Jenne, and M. Fioriono, 2001: The NCEP/NCAR 50-year reanalysis: Monthly means CD-ROM and documentation. Bull. Am. Meteorol. Soc., 82, 247–267

Marcos, M. and Tsimplis, M. N., 2008. Coastal sea level trends in Southern Europe. Geophysical Journal International, 175: 70–82. doi: 10.1111/j.1365-246X.2008.03892.x

Mariotti, A, Struglia, M. V., Zeng, N. and Lau, K-M., 2002: The Hydrological Cycle in the Mediterranean Region and Implications for the Water Budget of the Mediterranean Sea. J. Climate, 15, 1674–1690.

Raicich, F., N. Pinardi, A. Navarra, 2003. Teleconnections between Indian monsoon and Sahel precipitation and the Mediterranean.Int. J. Clim., 23, 173-186

Suselj, Kay, Tsimplis, Michael N., Bergant, Klemen, 2008. Is the Mediterranean Sea surface height variability predictable? Phys.And Chem. Of the Earth, 33, 3-4, 225-238 DOI: 10.1016/j.pce.2006.12.001

Tsimplis MN, Baker TF (2000). Sea level drop in the Mediterranean Sea: an indicator of deep water salinity and temperature changes. Geophys. Res. Lett. 27(12):1731-1734.

Tsimplis, M.N. and S.A. Josey, 2001. Forcing of the Mediterranean Sea by Atmospheric Oscillations over the North Atlantic. Geophysical Research Letters,28(5), 803-806.

Tsimplis, M.N., A.G.P. Shaw, 2008. The forcing of mean sea level variability around Europe. Global and Planetary Change 63, 196–202, doi:10.1016/j.gloplacha.2007.08.018.

Tsimplis, M.N. and M. Rixen, 2002, Sea Level in the Mediterranean Sea: The contribution of temperature and salinity changes, Geophys. Res. Let.,29(23), 2136-2140.

Tsimplis, M., Shaw, A., Flather, R. and Woolf, D. 2006. The influence of the North Atlantic Oscillation on the sea level around the northern European coasts reconsidered: the thermosteric effects. Phil. Trans. R. Soc. A.364(1841), 845–856.

Tsimplis, M. N., F. M. Calafat, M. Marcos, G. Jordà, D. Gomis, L. Fenoglio-Marc, M. V. Struglia, S. A. Josey, and D. P. Chambers (2013), The effect of the NAO on sea level and on mass changes in the Mediterranean Sea, J. Geophys. Res. Oceans, 118, doi:10.1002/jgrc.20078.

Volkov, D. L., G. Larnicol, and J. Dorandeu (2007), Improving the quality of satellite altimetry data over continental shelves, J. Geophys. Res., 112, C06020, doi:10.1029/2006JC003765.

Woodworth, P.L., Player, R., 2003. The permanent service for mean sea level: an update to the 21st century. J. Coast. Res. 19 (2), 287–295.

Tables

Table 1. List of tide gauges, location, periods of operation and percentage of gaps

Station Name	***Area***	***Latitude (º, Minutes)***	***Longitude (º, Minutes)***	***Period***	***Gaps (%)***
Malaga	W. Med.	36 43 N	04 25 W	1950-2010	15.00
Alicante	W. Med.	38 20 N	00 29 W	1960-1997	2.70
Marseille	W. Med.	43 18 N	05 21 E	1950-2011	0.00
Genova	W. Med.	44 24 N	08 54 E	1950-1997	6.38
Venice	Adriatic	45 26 N	12 20 E	1950-2000	2.00
Trieste	Adriatic	45 39 N	13 45 E	1950-2011	1.64
Rovinj	Adriatic	45 05 N	13 38 E	1955-2008	1.89
Bakar	Adriatic	45 18 N	14 32 E	1950-2008	1.72
Split I	Adriatic	43 30 N	16 23 E	1952-2008	1.79
Split II	Adriatic	43 30 N	16 26 E	1954-2008	1.85
Dubrovnik	Adriatic	42 40 N	18 04 E	1956-2008	1.92
Alexandria	E. Med.	31 13 N	29 55 E	1950-1989	2.56

Table 2. Correlation coefficients between winter (upper right triangle of the matrix) and summer (lower left triangle of the matrix, in italic) climate indices for the period 1950-2012. Boldface values denote statistical significance at 95% level.

	NAO	*EA*	*EA/WR*	*SCAN*
NAO	1.00	0.11	0.05	**-0.42**
EA	*-0.20*	1.00	0.02	0.00
EA/WR	*0.20*	***-0.37***	1.00	-0.16
SCAN	*0.17*	***-0.27***	***0.25***	1.00

Table 3. Mean and standard deviation of winter and summer variance of each data set. For tide gauges and atmospherically-corrected tide gauges the variance of each tide gauge was calculated and then the average value and the STD are shown. For sea level altimetry, DAC-Altimetry, atmospheric component, pressure-only and wind-only components and thermosteric sea level the variance at each grid point has been calculated and then the average and STD are shown. The lowest and highest variances of each data set are also shown (in brackets). (*) The units for the thermosteric rate of change are cm/month.

	Winter Variance (cm2)	*Summer Variance (cm2)*
Tide gauges	32±10 (17-44)	7±2 (2-10)
Atm-Corr. Tide gauges	11±2 (5-15)	5±2 (1-10)
Altimetry	19±7 (6-73)	6±6 (1-64)
DAC-Altimetry	11±7 (3-81)	6±6 (1-63)
Atmospheric component	6.1±2.1 (2.2-13.7)	0.6±0.1 (0.2-1.2)
Pressure-only component	3.3±1.5 (0.5-6.3)	0.4±0.1 (0.1-0.6)
Wind-only component	0.7±0.2 (0.4-2.8)	0.1±0.0 (0.1-0.4)
Thermosteric component	0.9±0.5 (0.0-2.5)	1.5±0.8 (0.0-4.6)
Thermost. rate of change*	0.2±0.1 (0.0-0.5)	0.4±0.1 (0.0-0.5)

Table 4. The percentage of the variance accounted for by each climatic index at each tide gauge for winter (above) and summer (below) for a regression model in which only one index is the independent parameter. In brackets the corresponding variance for the multiple regression model.

Variance accounted for

	Winter sea level				***Winter atmospherically-corrected sea level***			
Station	***NAO***	***EA***	***EA/WR***	***SCAN***	***NAO***	***EA***	***EA/WR***	***SCAN***
Málaga	40 (40)	3 (0)	0 (0)	1 (0)	7 (0)	4 (0)	4 (0)	1 (0)
Alicante	47 (47)	5 (0)	0.4 (0)	7 (0)	20 (15)	14 (9)	0 (0)	2 (0)
Marseille	32 (29)	10 (7)	1 (0)	12 (0)	10 (7)	22(18)	0 (0)	4 (0)
Genova	44 (43)	10 (0)	8 (6)	24 (0)	19 (14)	19 (14)	0 (0)	8 (0)
Venice	24 (13)	1(0)	25(18)	25 (9)	14 (0)	5 (0)	26 (19)	21 (14)
Trieste	33 (33)	5 (0)	20 (20)	20 (0)	14 (11)	9 (6)	15 (14)	7 (0)
Rovinj	35 (26)	5 (0)	16 (14)	22 (5)	18 (16)	11 (7)	11 (11)	11 (0)
Bakar	32 (32)	4 (0)	22 (22)	19 (0)	18 (18)	6 (0)	17 (17)	7 (0)
Split 1	39 (39)	1 (0)	17 (17)	18 (0)	24 (24)	3 (0)	9 (9)	7 (0)
Split 2	39 (39)	2 (0)	15 (15)	18 (0)	21 (21)	5 (0)	8 (8)	7 (0)
Dubrovnik	40 (40)	0 (0)	17 (17)	18 (0)	26 (26)	2 (0)	14 (14)	12 (0)
Alexandria	17 (16)	1 (0)	16 (15)	0 (0)	7 (0)	2 (0)	14 (14)	2 (0)

	Summer sea level				***Summer atmospherically-corrected sea level***			
	NAO	***EA***	***EA/WR***	***SCAN***	***NAO***	***EA***	***EA/WR***	***SCAN***
Málaga	3 (0)	2 (0)	7 (0)	1 (0)	3 (0)	4 (0)	8 (0)	0 (0)
Alicante	0 (0)	1 (0)	0 (0)	18 (18)	0 (0)	4 (0)	0 (0)	7 (0)
Marseille	2 (0)	6 (0)	0 (0)	2 (0)	1 (0)	11 (11)	0 (0)	0 (0)
Genova	3 (0)	16 (16)	2 (0)	0 (0)	0 (0)	14 (14)	2 (0)	2 (0)
Venice	5 (0)	6 (0)	6 (0)	1 (0)	2 (0)	6 (0)	5 (0)	0 (0)
Trieste	15 (15)	8 (0)	5 (0)	1 (0)	10 (0)	13 (13)	7 (0)	0 (0)
Rovinj	13 (10)	11 (8)	5 (0)	0 (0)	7 (0)	16 (16)	7 (0)	1 (0)
Bakar	13 (13)	7 (0)	4 (0)	0 (0)	6 (0)	9 (9)	5 (0)	1 (0)
Split 1	14 (14)	10 (0)	5 (0)	0 (0)	11 (1)	14 (11)	6 (0)	2 (0)
Split 2	15 (15)	10 (0)	2 (0)	0 (0)	11 (7)	15 (11)	2 (0)	2 (0)
Dubrovnik	5 (0)	5 (0)	2 (0)	0 (0)	4 (0)	8 (8)	3 (0)	2 (0)
Alexandria	2 (0)	0 (0)	1 (0)	1 (0)	1 (0)	0 (0)	1 (0)	2 (0)

Table 5. Correlation coefficients and the variance accounted for, by the regression model in which each climate index has been regressed against the corresponding sea level parameter. Results for winter are shown. The variance accounted for by the multiple regression model is shown in brackets. Boldface values denote statistically significance at 95% level. Western and Eastern Mediterranean values are also shown.

		NAO		*EA*		*EA/WR*		*SCAN*	
		Corr	*EV (%)*	*Corr*	*EV (%)*	*Corr*	*EV (%)*	*Corr*	*EV (%)*
Altimetry	*Med*	**-0.91**	83 (77)	0.10	1 (0)	**-0.36**	13 (7)	**0.75**	56 (0)
	WMed	**-0.90**	81 (76)	0.19	4 (0)	**-0.35**	12 (7)	**0.78**	61 (0)
	EMed	**-0.89**	79 (73)	0.08	1 (0)	**-0.36**	13 (7)	**0.73**	53 (0)
DAC Altimetry	*Med*	**-0.89**	79 (79)	0.26	7 (0)	-0.20	4 (0)	**0.57**	32 (0)
	WMed	**-0.80**	64 (52)	**0.49**	24 (12)	-0.05	0 (0)	**0.48**	23 (0)
	EMed	**-0.89**	79 (79)	0.21	4 (0)	-0.23	5 (0)	**0.60**	36 (0)

Table 6. Correlation coefficients and the variance accounted for, by the regression model in which each climate index has been regressed against the atmospherically-induced sea level, pressure only-induced sea level and wind only-induced sea level. Results for winter (above) and summer (below) are shown. The variance accounted for by the multiple regression model is shown in brackets. Boldface values denote statistically significance at 95% level. Western and Eastern Mediterranean values are also shown.

		NAO		***EA***		***EA/WR***		***SCAN***	
		Corr	***EV (%)***	***Corr***	***EV (%)***	***Corr***	***EV (%)***	***Corr***	***EV (%)***
Winter Atmospheric	***Med***	**-0.71**	50 (50)	-0.01	0 (0)	**-0.32**	10 (11)	**0.47**	22 (0)
	Wmed	**-0.73**	53 (42)	0.03	0 (0)	**-0.26**	7 (5)	**0.49**	24 (4)
	Emed	**-0.67**	45 (45)	-0.04	0 (0)	**-0.35**	12 (13)	**0.43**	18 (0)
Winter Pressure-only	***Med***	**-0.68**	46 (49)	-0.12	1 (4)	**-0.33**	11 (12)	**0.47**	22 (0)
	Wmed	**-0.70**	49 (38)	-0.06	0 (0)	**-0.30**	9 (7)	**0.51**	26 (5)
	Emed	**-0.63**	39 (44)	-0.15	2 (6)	**-0.35**	12 (13)	**0.4**	16 (0)
Winter Wind-only	***Med***	**-0.67**	45 (45)	0.21	4 (0)	-0.25	6 (7)	**0.42**	18 (0)
	Wmed	**-0.67**	45 (45)	**0.28**	8 (0)	-0.10	1 (0)	**0.34**	12 (0)
	Emed	**-0.65**	42 (42)	0.17	3 (0)	**-0.30**	9 (9)	**0.44**	19 (0)

		NAO		***EA***		***EA/WR***		***SCAN***	
		Corr	***EV (%)***	***Corr***	***EV (%)***	***Corr***	***EV (%)***	***Corr***	***EV (%)***
Summer Atmospheric	***Med***	-0.19	4 (0)	-0.1	1 (0)	0.09	1 (0)	**0.38**	14 (14)
	Wmed	-0.09	1 (0)	-0.18	3 (0)	0.12	1 (0)	**0.41**	17 (17)
	Emed	-0.22	5 (8)	-0.07	0 (0)	0.07	0 (0)	**0.35**	12 (16)
Summer Pressure-only	***Med***	**-0.30**	9 (13)	0.03	0 (0)	0.04	0 (0)	**0.34**	12 (16)
	Wmed	-0.21	4 (8)	-0.08	1 (0)	0.09	1 (0)	**0.42**	18 (22)
	Emed	**-0.32**	10 (14)	0.07	0 (0)	0.02	0 (0)	**0.31**	10 (13)
Summer Wind-only	***Med***	0.14	2 (0)	**-0.31**	10 (10)	0.12	1 (0)	0.21	4 (0)
	Wmed	0.19	4 (0)	**-0.29**	8 (8)	0.13	2 (0)	0.18	3 (0)
	Emed	0.12	1 (0)	**-0.31**	10 (10)	0.12	1 (0)	0.22	5 (0)

Table 7. Correlation coefficients and the variance account for, by the regression model in which each climate index has been regressed against the thermosteric sea level and the monthly rate of change of thermosteric sea level. Results for winter are shown. Results for summer are shown only for the rate of change of thermosteric. The variance accounted for by the multiple regression model is shown in brackets. Boldface values denote statistically significance at 95% level. Western and Eastern Mediterranean values are also shown.

		NAO		***EA***		***EA/WR***		***SCAN***	
		Corr	***EV (%)***	***Corr***	***EV (%)***	***Corr***	***EV (%)***	***Corr***	***EV (%)***
Winter Thermosteric	***Med***	-0.23	5 (0)	-0.20	4 (0)	-0.04	0 (0)	**0.30**	9 (9)
	Wmed	-0.02	0 (0)	-0.10	1 (0)	0.05	0 (0)	0.15	2 (0)
	Emed	**-0.28**	8 (0)	-0.21	4 (6)	-0.06	0 (0)	**0.32**	10 (12)
Winter Rate of change	***Med***	-0.18	3 (0)	**0.49**	24 (17)	-0.22	5(4)	0.21	4 (0)
	Wmed	0.09	1 (0)	**0.44**	19 (16)	0.10	1 (0)	-0.14	2 (0)
	Emed	**-0.25**	6 (0)	**0.40**	16 (11)	**-0.30**	9 (6)	**0.30**	9 (4)
Summer Rate of Change	***Med***	0.06	0 (0)	0.13	2 (0)	**-0.35**	12 (12)	-0.19	3 (0)
	Wmed	-0.05	0 (0)	-0.06	0 (0)	-0.09	1 (0)	**-0.29**	9 (9)
	Emed	0.09	1 (0)	0.18	3 (0)	**-0.37**	14 (14)	-0.09	1 (0)

Table 8. Variance accounted for by the regression model in which each climate index has been regressed against the sea level and its components for the altimetry period (1993-2008). The variances of the altimetric sea level accounted for by the atmospheric and thermosteric components are also shown. Results for winter and summer are shown. The variance accounted for by the multiple regression model is shown in parentheses. The lowest and highest variances accounted for by each tide gauge are also shown for the altimetry period (in brackets).

	Altimetry		***DAC-Altimetry***		***Atmospheric component***		***Thermosteric component***		***Tide gauges***		***Atm-corrected tide gauges***	
	Win	***Sum***	***Win***	***Sum***	***Win***	***Sum***	***Win***	***Sum***	***Win***	***Sum***	***Win***	***Sum***
NAO (%)	86(86)	0(0)	72(72)	0(0)	70(0)	1(0)	2(0)	6(0)	[31-64] ([0 45])	[0-15]	[7-56] ([0-54])	[0-2](0)
EA (%)	0(0)	5(0)	1(0)	3(0)	3(0)	0(0)	0(0)	6(0)	[0-4] (0)	[0-16]	[2-14](0)	[0-7](0)
EA/WR (%)	1(0)	0(0)	0(0)	1(0)	2(0)	2(0)	19(0)	2(0)	[0-7](0)	0	[0-5](0)	[0-3] (0)
SCAN (%)	60(0)	0(0)	25(0)	1(0)	80(80)	10(0)	2(0)	0(0)	[10-65] ([0 63])	[0-18]	[1-37](0)	[0-5](0)
Atmospheric Component (%)	74	42	-	-	-	-	-	-	-	-	-	-
Thermosteric Component (%)	0	0	0	1	-	-	-	-	-	-	-	-

Figures

Figure 1. Winter (Dec-Mar) NCEP 2m air temperature anomalies (coloured field, ºC), 10m wind speed anomalies (vectors) and sea level pressure anomalies (contours) for a unit value of the positive index of: (a) NAO, (b) EA, (c) EA/WR and (d) SCAN. Note that the horizontal vector (red arrow) is for scale and indicates a wind speed of 5m/s.

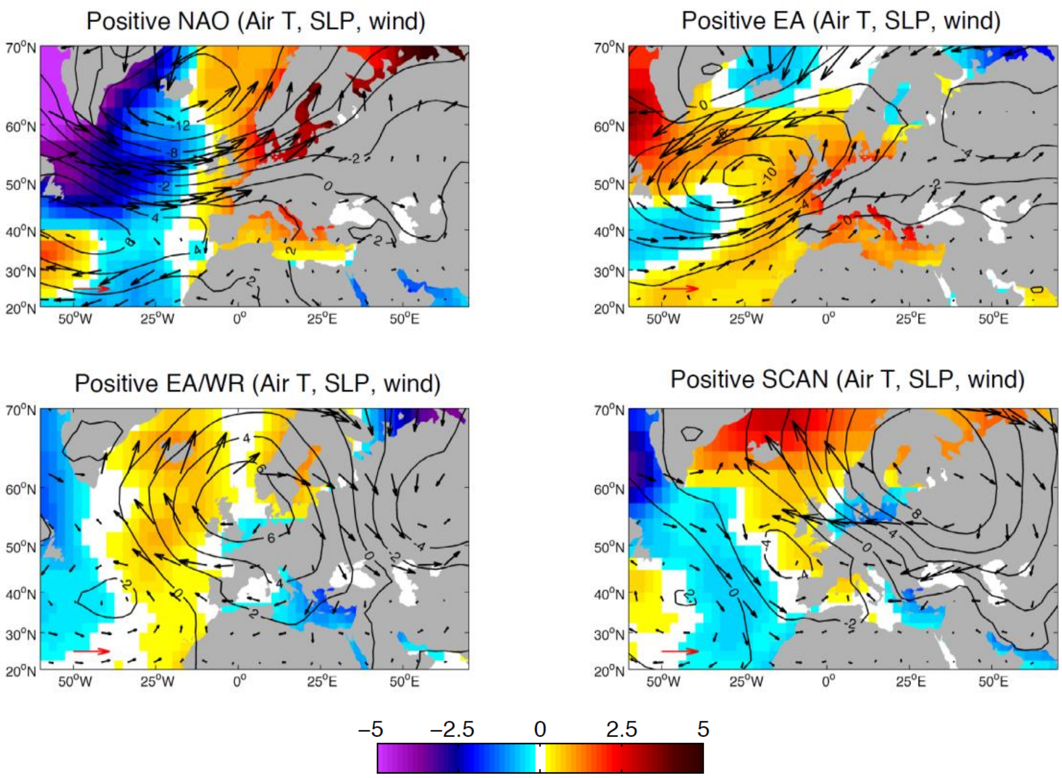

Figure 2. Dec-Mar (triangles and stars) and Jun-Aug (circles and squares) correlation coefficients between NAO (a), EA (b), EA/WR (c), SCAN (d) and tide gauges (black) and atmospherically corrected tide gauges (grey) for the common period 1958-2008. Filled symbols denote statistically significance at 95% level. Site names are listed in Table 1.

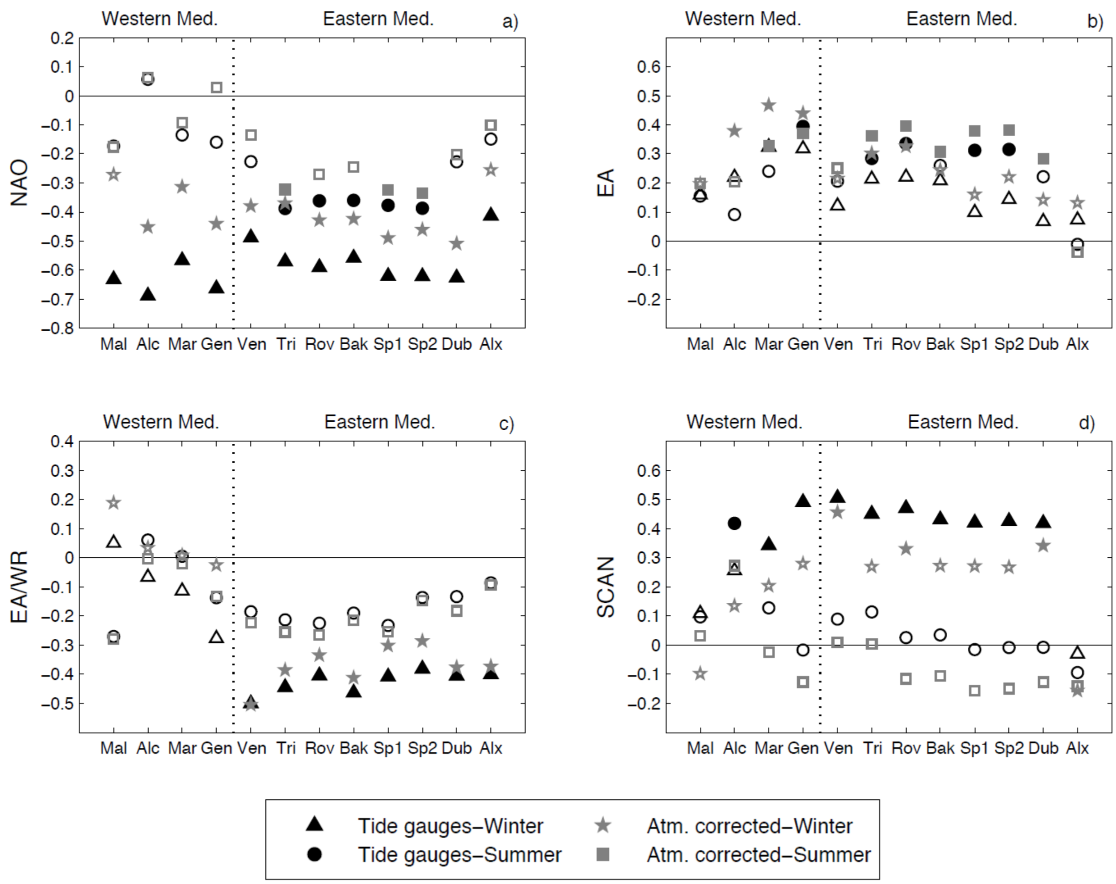

Figure 3. Winter (left) and summer (right) sea level at tide gauges (in grey) and time series reconstructed using the multiple regression model (black lines) with the corresponding indices (Figure 2 and Table 4).

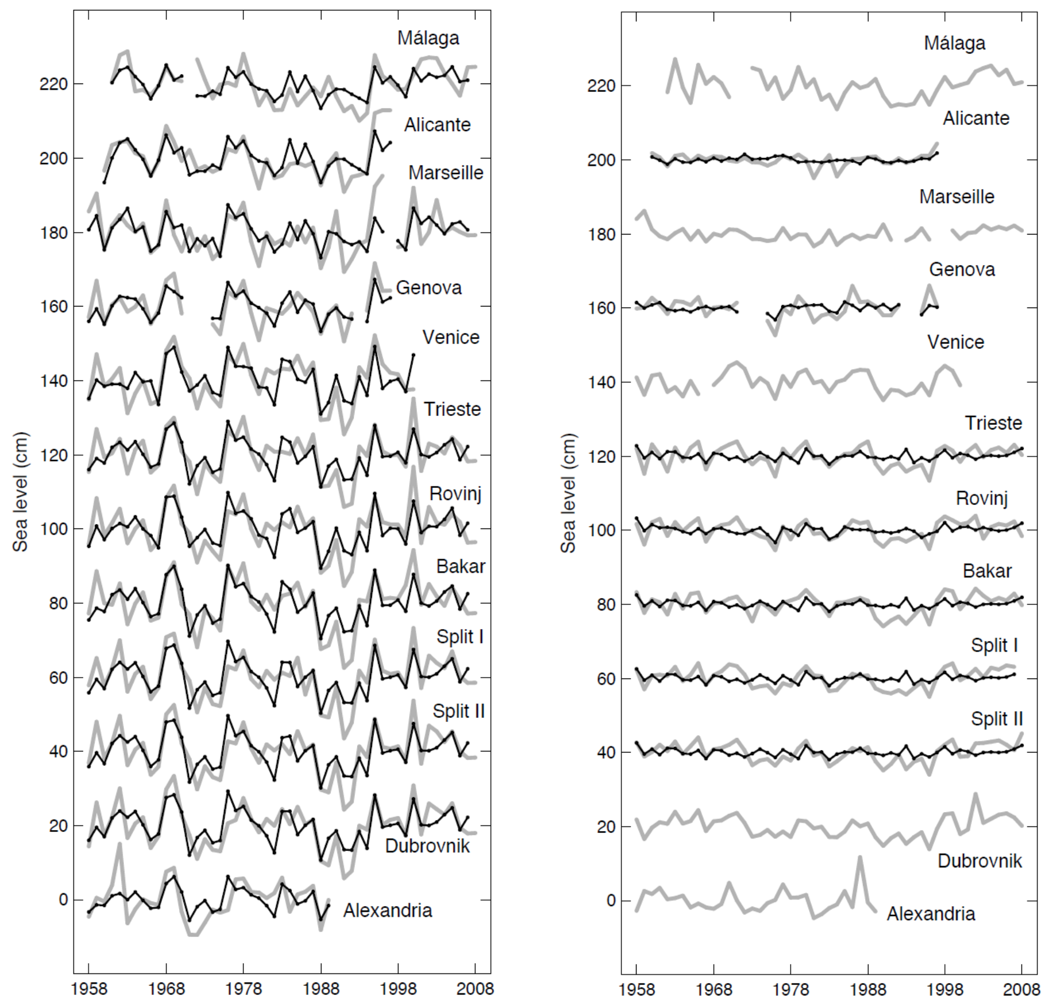

Figure 4. Maps of the correlation coefficient between winter climate indices and winter altimetry (left) and DAC-altimetry (right) for the period 1993-2010. Dotted areas denote significant correlation at 95% level. Correlations with tide gauges are also shown for the same period (coloured circles). Only those tide gauges longer than 10 years of data during 1993-2010 are shown.

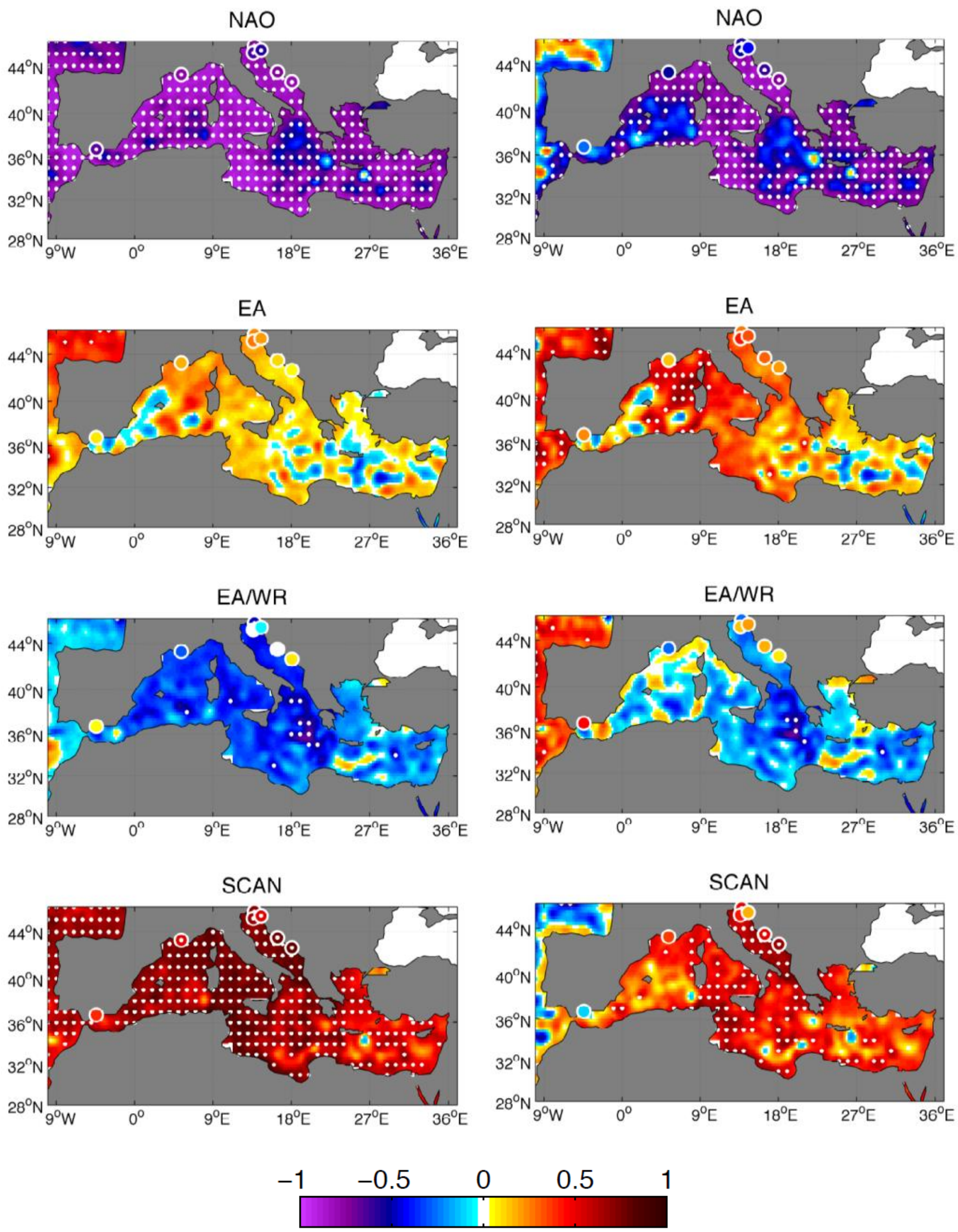

Figure 5. Overall contribution of independent modes to winter basin average altimetry (top) and winter basin average DAC-altimetry (bottom).

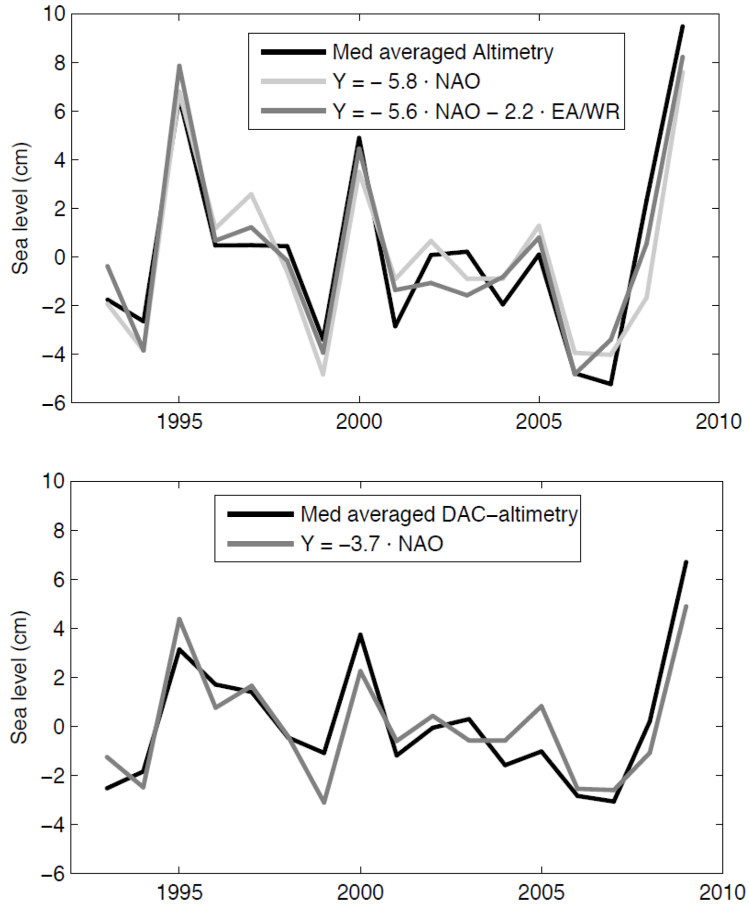

Figure 6. Dec-Mar and Jun-Aug maps of correlation coefficients between climate modes and atmospherically-induced sea level and wind-only induced sea level for the period 1958-2008. Dotted areas denote significant correlation at 95% level.

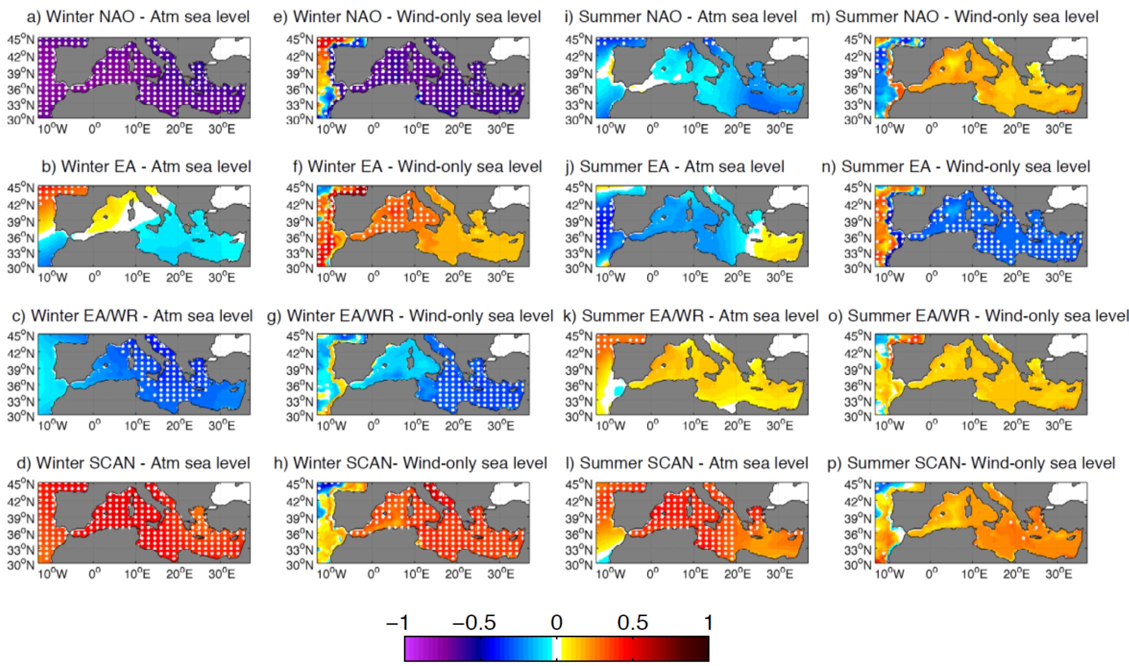

Figure 7. Overall contribution of independent modes to winter (top) and summer (bottom) basin average atmospherically induced sea level variability.

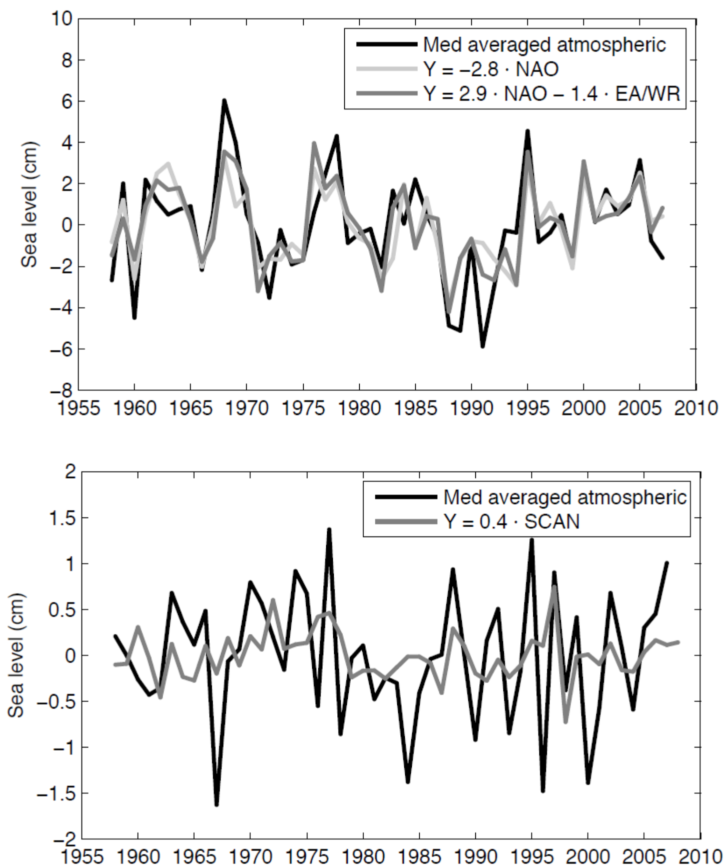

Figure 8. Dec-Mar and Jun-Aug maps of correlation coefficients between the climate indices and the thermosteric sea level (left) and the rate of change of thermosteric sea level (center and right) for the period 1950-2011. Dotted areas denote significant correlation at 95% level.

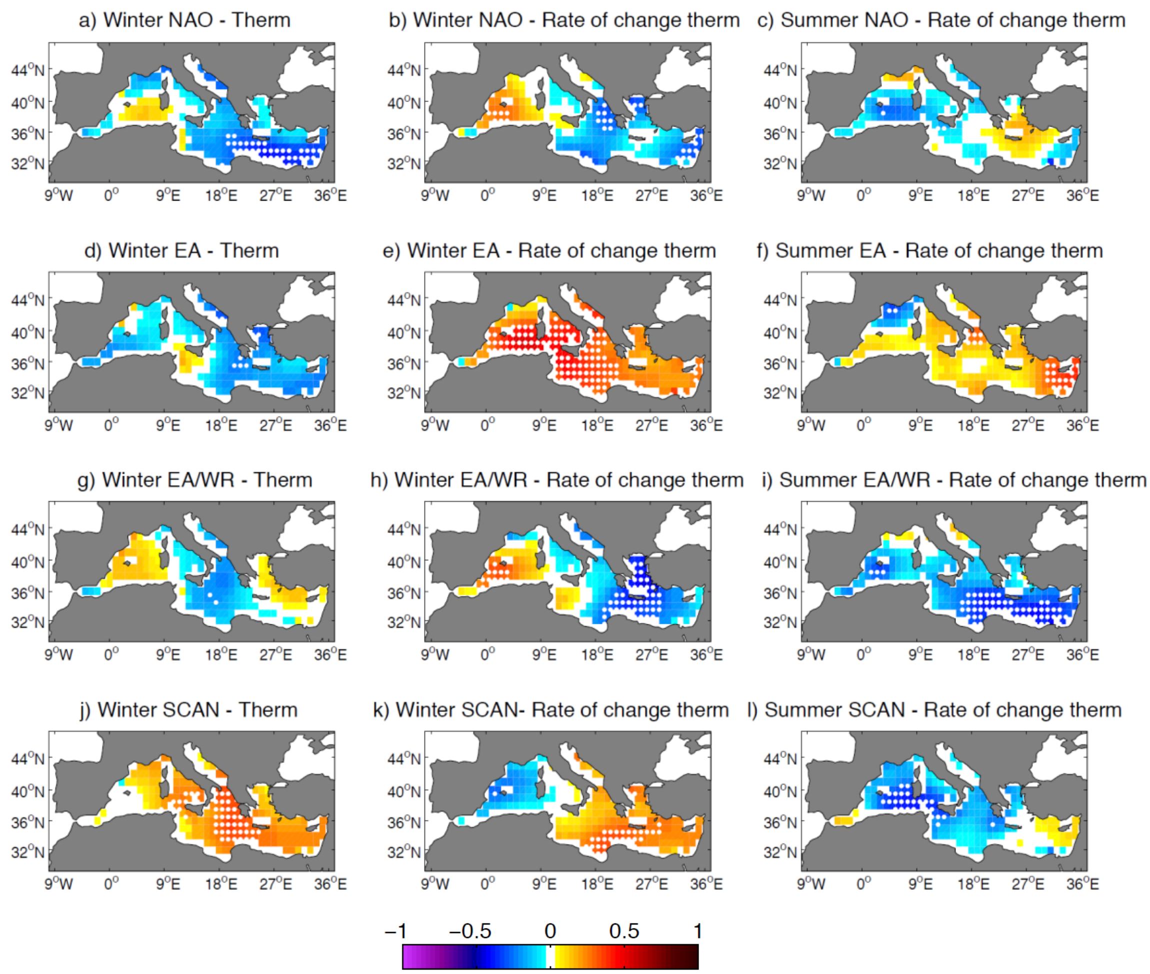

Figure 9. Dec-Mar contribution of the SCAN to the winter basin averaged thermosteric sea level. Averaged thermosteric sea level of the highest correlated area is also shown for comparison (light-grey line).

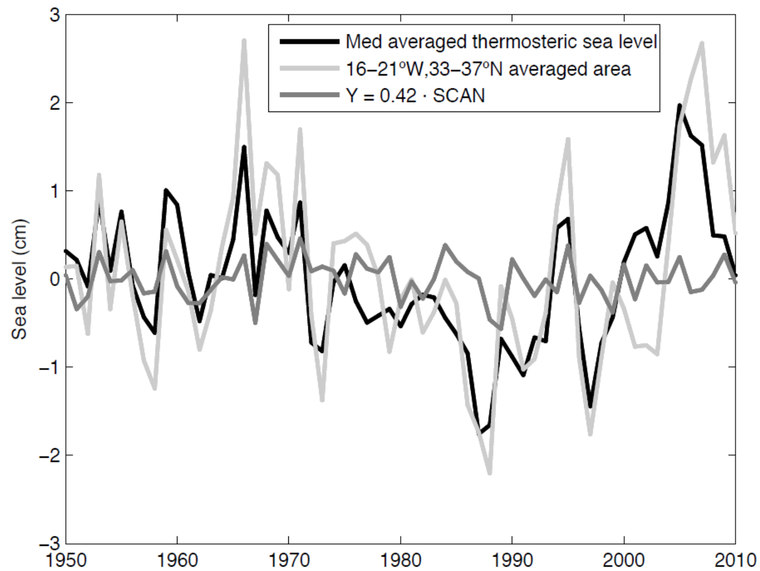

Figure 10. Winter (Dec-Mar) atmospherically-induced sea level (cm) and 10m wind speed (vectors) averaged for a winter NAO (top) and EA/WR (bottom) indices: (a,c) positive state, (b,d) negative state. Corresponding averaged sea level pressures are contoured in intervals of 1 mb. Note that the horizontal vector (red arrow) is for scale and indicates a wind speed of 2m/s.

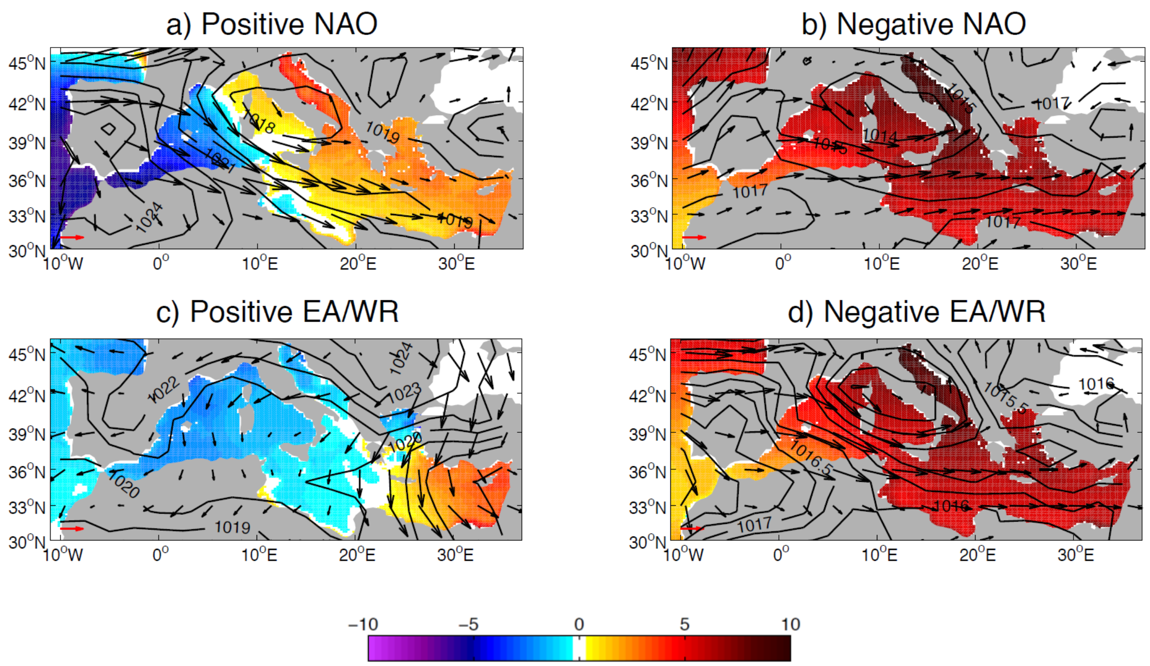

Figure 11. Winter (Dec-Mar) rate of change of thermosteric sea level anomalies (cm) and 10m wind speed (vectors) averaged for winter NAO (a,b), EA (c,d), EA/WR (e,f) and SCAN (g,h) indices under a positive state (left) and a negative state (right). Corresponding averaged sea level pressures are contoured in intervals of 1 mb. Note that the horizontal vector (red arrow) is for scale and indicates a wind speed of 2m/s.

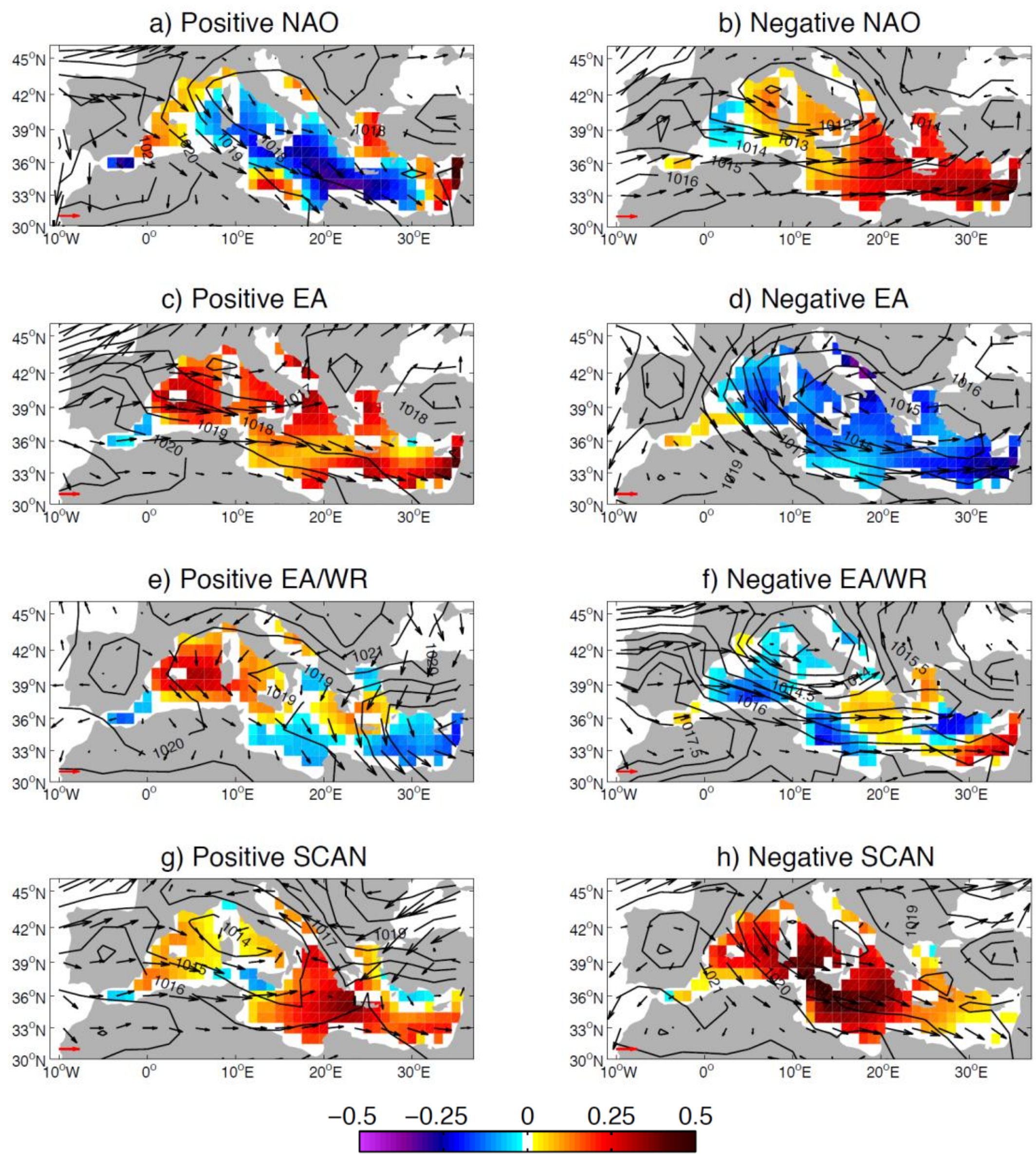

Figure 12. Summer (Jun-Aug) atmospherically induced sea level (cm) averaged for a summer SCAN positive and negative phases (above). Rate of change of thermosteric sea level anomalies (cm) averaged for a summer EA/WR positive and negative phases (below). Corresponding 10m wind speed (vectors) and sea level pressure are contoured in intervals of 1 mb. Note that the horizontal vector above Figure 12a is for scale and indicates a wind speed of 2m/s.